Journal of
Water & Climate Change

Check for updates

IWA PUBLISHING

© 2024 The Authors

Journal of Water and Climate Change Vol 15 No 3, 1172 doi: 10.2166/wcc.2024.520

Forecasting of water quality parameters of Sandia station in Narmada basin, Central India, using AI techniques

Deepak Kumar Tiwari [a,*], K. R. Singh[a] and Vijendra Kumar [b]

[a] Department of Civil Engineering, GLA University, Matura, Uttar Pradesh 281406, India
[b] Department of Civil Engineering, Dr Vishwanath Karad MIT World Peace University, Pune, Maharashtra 411038, India
*Corresponding author. E-mail: deepaktiwaricivil7sept@gmail.com, deepak.tiwari@gla.ac.in

DKT, 0000-0002-9253-1153; VK, 0000-0002-0053-1210

ABSTRACT

In addition to the influence of climate change on water availability and hydrological risks, the effects on water quality are in the early stages of investigation. This study aims to consolidate the latest interdisciplinary research in the application of artificial intelligence (AI) in the field of assessment of water quality parameters and its prediction. This research paper specifically explores the intricate relationship between climate change and water quality parameters at Sandia station, situated within the Narmada basin in Central India. As global climatic patterns continue to shift, the repercussions on water resources have gained prominence. In this work, electrical conductivity is predicted using the KERAS data processing environment on TensorFlow. The root-mean-square error (RMSE), coefficient of determination (R^2), Nash–Sutcliffe efficiency (NSE), etc. are calculated between observed and predicted values to assess the model performance. A total of ten models are developed depending upon the input geometry from past monthly timelines. The results indicate that model 8, with ten inputs, performs the best based on the R^2 value of 0.889. These results indicate that AI can be very helpful in analyzing the possible threats in the future for drinking water, livestock feeding, irrigation, and so on.

Key words: ANN, climate change, electrical conductivity, Keras, water quality

HIGHLIGHTS

- Long short-term memory (LSTM) models used for prediction of water quality.
- Unique study of electrical conductivity in the central part of India.
- Study of impacts of climate change on India based on water quality parameters.
- Study is carried out at Sandia Hydrological site.
- Five performance efficiency parameters used to calculate predicting capability.

This is an Open Access article distributed under the terms of the Creative Commons Attribution Licence (CC BY 4.0), which permits copying, adaptation and redistribution, provided the original work is properly cited (http://creativecommons.org/licenses/by/4.0/).

Downloaded from http://iwaponline.com/jwcc/article-pdf/15/3/1172/1394322/jwc0151172.pdf
by guest

GRAPHICAL ABSTRACT

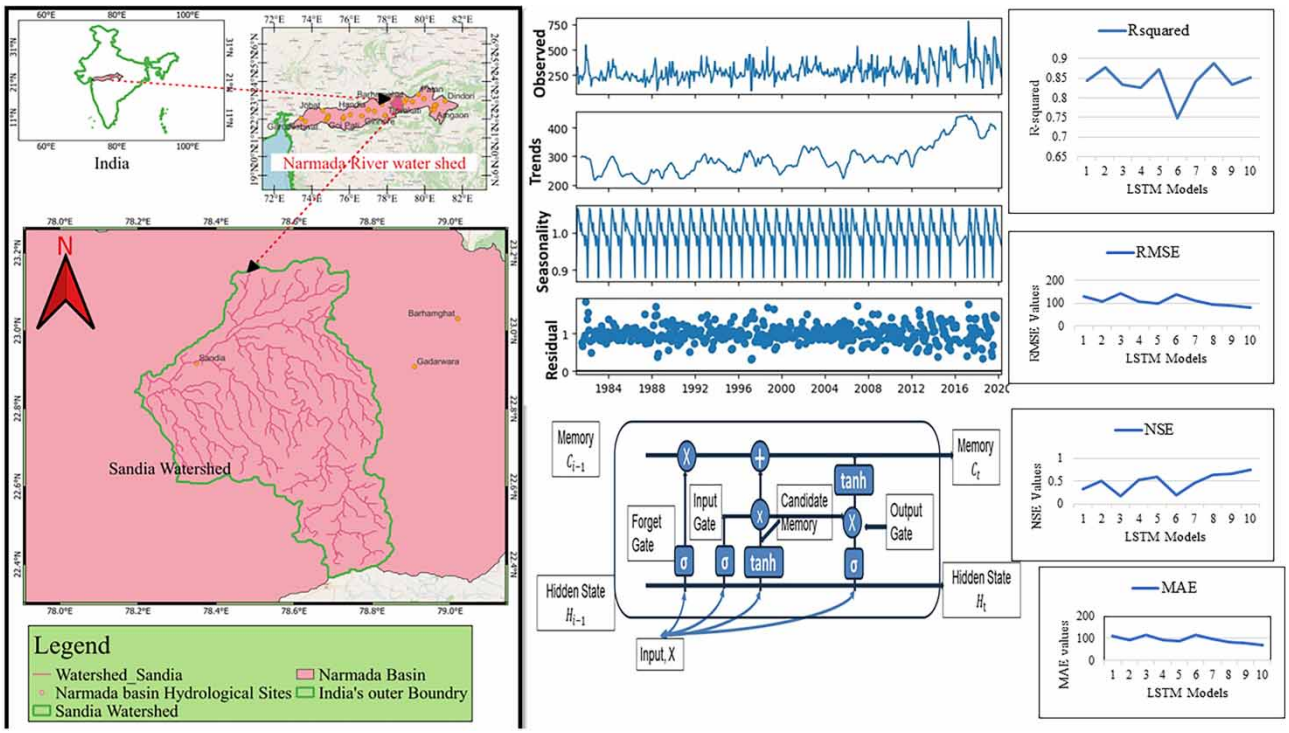

INTRODUCTION

The primary consequences of climate change on water availability manifest as floods and droughts, which are highly devastating extreme events (Goyal & Surampalli 2018). In addition to these quantitative shifts, climate change also exerts an influence on the quality of surface water (Tiwari *et al.* 2022). For instance, it is apparent that drought conditions can inevitably trigger alterations in the concentration and quality of surface or subsurface water, occasionally resulting in constraints on water supply (Delpla *et al.* 2009; Mishra & Nagarajan 2010; Mohammed & Scholz 2018; Kumar *et al.* 2021). While the deterioration of water quality can directly impact the extraction of surface water, wells might need to be discontinued because of concerns about both groundwater quality and safety issues associated with flooding risks (Doocy *et al.* 2013). However, despite the general acknowledgment of these realities, only a limited number of scientific studies have been previously available that delved into the ramifications of climate change on modifications to water quality. The overarching observation is that the decline in drinking water quality, prompted by the context of climate change, accentuates the prevalence of situations that pose potential health risks (Rai & Singh 2015; Dile *et al.* 2018; Van Allemann *et al.* 2019). Central India is also vulnerable to the extreme conditions of climate and anthropogenic activities that not only degrade the quality of potable water but also pose a threat to the flora and fauna. Narmada River is in the central part of India. The Narmada basin, also located in Central India, is a vital water resource region that sustains the livelihoods of millions while supporting diverse ecosystems. The Narmada River serves as a lifeline, providing water for irrigation, domestic use, and industrial activities (Bhagwat & Maity 2014). However, the Narmada basin water resources are under constant increasing pressure due to the mounting impact of climate change. With the rise in global temperature and the emergence of unpredictable weather patterns, an imbalance has been created between natural systems that dramatically affects the water quality of the river (Corwin & Lesch 2005; Mauser & Bach 2009; Kumar 2016; Heddam & Kisi 2018).

Electrical conductivity (EC) of water is generally referred to as the ability of the water body to allow the passage of electric current through it. The health of water bodies is affected by the quantity of EC present (Pal *et al.* 2015). EC helps monitor the salinity of irrigation water, which is added to the soil and affects the health of plants and crop yield (Corwin & Lesch 2005). Water stress conditions are observed in plants because of high salinity content. EC also helps in detection of the mixing of ground water and surface water and the movements of water molecules. Sources of water can also be tracked down with the

Downloaded from http://iwaponline.com/jwcc/article-pdf/15/3/1172/1394322/jwc0151172.pdf
by guest

help of this tool and it helps in understanding the flow hydraulics (Lau *et al.* 2019). Subsurface materials have some properties that can also be indicated with the help of EC. In addition to salinity, EC can also indicate the presence of contaminants like heavy metals or pollutants in water (Gomaa *et al.* 2020). Overall, EC is a versatile parameter that offers valuable information about the electrical properties of materials, aiding in various scientific, industrial, and environmental applications. But the measurement and prediction of EC is quite challenging and efficient models are difficult to train in data-scarce regions of South Asian countries.

Furthermore, the specific influence of climate changes on water quality in the Narmada basin remains understudied. This study endeavors to bridge this gap by investigating how climate change impacts EC as a water quality parameter at Sandia station. The findings of this study hold implications not only for the Narmada basin but also for broader water resource management strategies in the face of climate change. By unraveling the complexities of this relationship, the paper contributes to a deeper understanding of the potential challenges posed by climate-induced alterations in water quality, ultimately aiding in the formulation of informed mitigation and adaptation strategies. Also, the paper has examined how alterations in the properties of the physicochemical parameters affect the quality of water resources like rivers and lakes. Subsequently, the discussion delves into the projected implications for the production of potable water and the quality of the supplied water. In this paper, a novel method is proposed to predict the EC on a monthly scale by using the Keras software which uses TensorFlow environment packages. Keras is an application programming interface (API) designed for human beings, not machines. It follows best practices for reducing cognitive load: it offers consistent and simple APIs, minimizes the number of user actions required for common use cases, and provides clear and actionable error messages. Keras also gives the highest priority to crafting great documentation and developer guides. The models are trained and tested first. After that, these trained models are used for predictions. A total of ten models were analyzed, each having between three and 12 hidden layers. The models' performances are then compared based on various efficiency parameters such as the root-mean-square error (RMSE), and so on. Overall, these models are promising tools in the field of predicting EC on a pre-monthly basis and to make sound and informed decisions based on this knowledge. The reader will gain new insights with this work about the application of artificial intelligence (AI) in the field of water quality parameter prediction with the help of the long short-term memory (LSTM) technique, which is a new and innovative method that has very good accuracy.

Study area

Sandia is a village located in the Indian state of Madhya Pradesh. It lies in the Hosangabad district, in the central region of India. It is 85 km southwest of Hosangabad and 120 km southeast of Bhopal. Figures 1 shows the study area of Sandia catchment of Narmada River. Diverse geological features such as forests, water bodies, barren land, residential area, and agricultural land are part of the Sandia watershed. Apart from agriculture, the local economy also includes small-scale businesses, shops, and services catering to the needs of the community. It is advisable to refer to official government sources and local authorities, or conduct field studies, for more detailed and up-to-date insights into the area. Sandia has a total watershed area of 3,367.7 km^2. It experiences a subtropical climate, which is characterized by distinct seasons. The summer months in Sandia are typically hot and dry. Temperatures can soar above 40 °C (104 °F) during the peak of summer. This period is marked by intense heat and a portion of its annual rainfall during the monsoon season. Monsoon rains bring relief from the scorching heat and contribute to the region's agricultural activities. However, heavy rains can also lead to localized flooding. Sandia receives significant rainfall during monsoon season (July to September). After the monsoon season, temperatures begin to gradually decrease, and the weather becomes more pleasant. This is a transitional period. Winters in Sandia are relatively mild, with temperatures ranging from 10 to 20 °C (50–68 °F). It is a comfortable time for outdoor activities. The monsoon season, with its heavy rainfall, significantly contributes to the water resources in the region. Adequate water management is crucial for harnessing and utilizing this resource effectively.

Data collection

Monthly data on EC are obtained from the Central Water Commission (CWC) Bhopal for the Sandia site. The detailed data statistics related to EC are provided in Tables 1 and 2. The dataset exhibits several key statistical properties. The mean value of the data is approximately 293.71 μmho/cm, with a standard error of 4.44. The median, which represents the middle value in the dataset, is 277 μmho/cm, while the mode, indicating the most frequently occurring value, is 227 μmho/cm. The standard deviation, a measure of data dispersion, is approximately 96.93, and the sample variance is 9,394.50. The kurtosis value is 2.10, indicating a relatively peaked distribution, while the skewness value is 1.19, suggesting a slightly right-skewed

Downloaded from http://iwaponline.com/jwcc/article-pdf/15/3/1172/1394322/jwc0151172.pdf
by guest

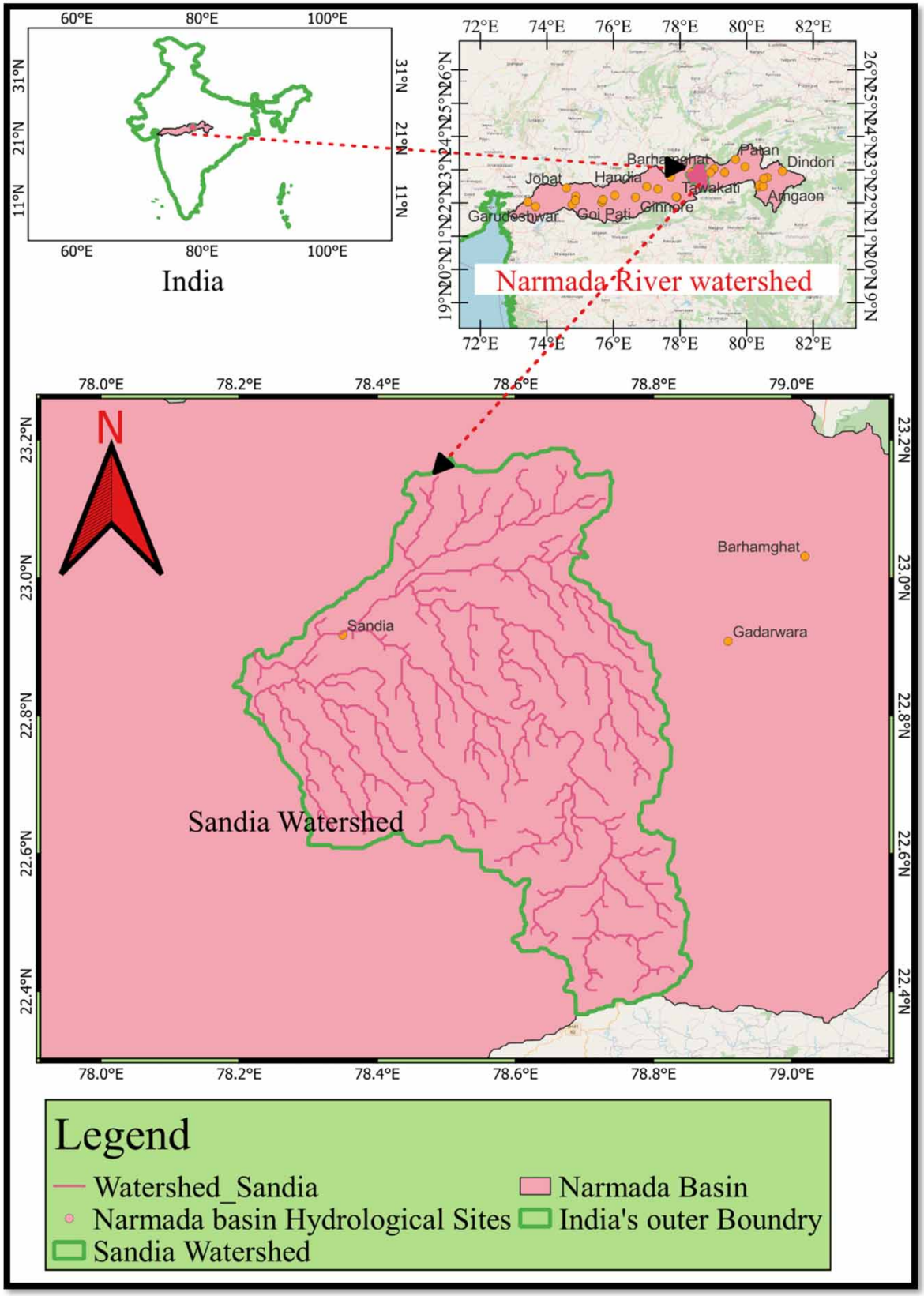

Figure 1 | Sandia watershed on Narmada River basin.

Downloaded from http://iwaponline.com/jwcc/article-pdf/15/3/1172/1394322/jwc0151172.pdf
by guest

Table 1 | Electrical conductivity descriptive statistics for Sandia hydrological site (μmho/cm)

Mean	Standard error	Median	Mode	Standard deviation	Sample variance
293.7143	4.437902	277	227	96.92524	9,394.502

Table 2 | Electrical conductivity data statistics for Sandia hydrological site (μmho/cm)

Kurtosis	Skewness	Range	Minimum	Maximum	Confidence level (95.0%)
2.096373	1.189028	682	98	780	8.720301

distribution. The range, which represents the difference between the maximum (780 μmho/cm) and minimum (98 μmho/cm) values in the dataset, is 682 μmho/cm. With a 95% confidence level, we can infer that the true population parameters are within a certain range, with a margin of error of approximately ± 8.72 around the sample mean of 293.71 μmho/cm. Figures 2 and 3 represent the temporal variation in EC data, trends, and seasonality presented in values.

The EC monthly data at the Sandia hydrological site on the Narmada River has been decomposed into four distinct components: observed, trend, seasonality, and residual. The observed component represents the actual measured EC values for each month. It includes all the variations and fluctuations in the data, which can be influenced by a variety of factors such as weather, environmental changes, and human activities. The trend component captures the long-term changes or patterns in the EC data. It indicates that there is a consistent increase in conductivity over time.

The seasonality component reveals regular fluctuations that occur as a result of seasonal factors such as rainfall, temperature, or agricultural practices. Lastly, the variability present in data that can neither be associated with trend nor with seasonality is represented as residuals. The residuals incorporate random fluctuations and unexplained variations, which could be triggered by errors occurring during measurement of EC or by unpredictable factors. The decomposition of the data into these four components helped the research work in better understanding the fundamental patterns and causes of variation in EC at the Sandia hydrological site, which in turn helped in making better-informed decisions and identifying potential environmental trends or issues.

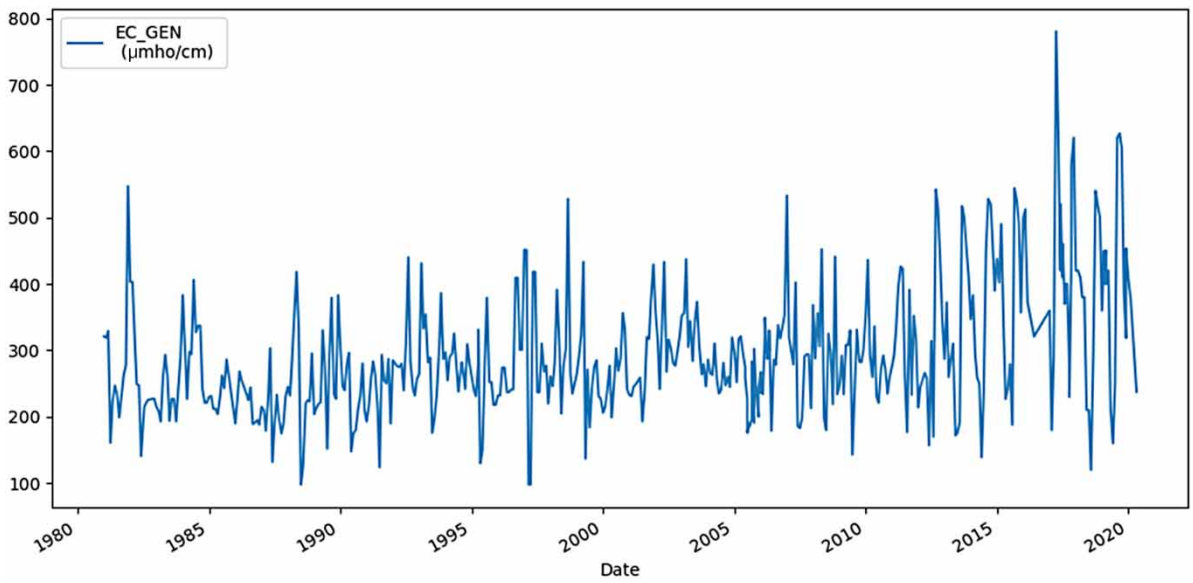

Figure 2 | Electrical conductivity monthly data from the Sandia hydrological site, Narmada River.

Downloaded from http://iwaponline.com/jwcc/article-pdf/15/3/1172/1394322/jwc0151172.pdf
by guest

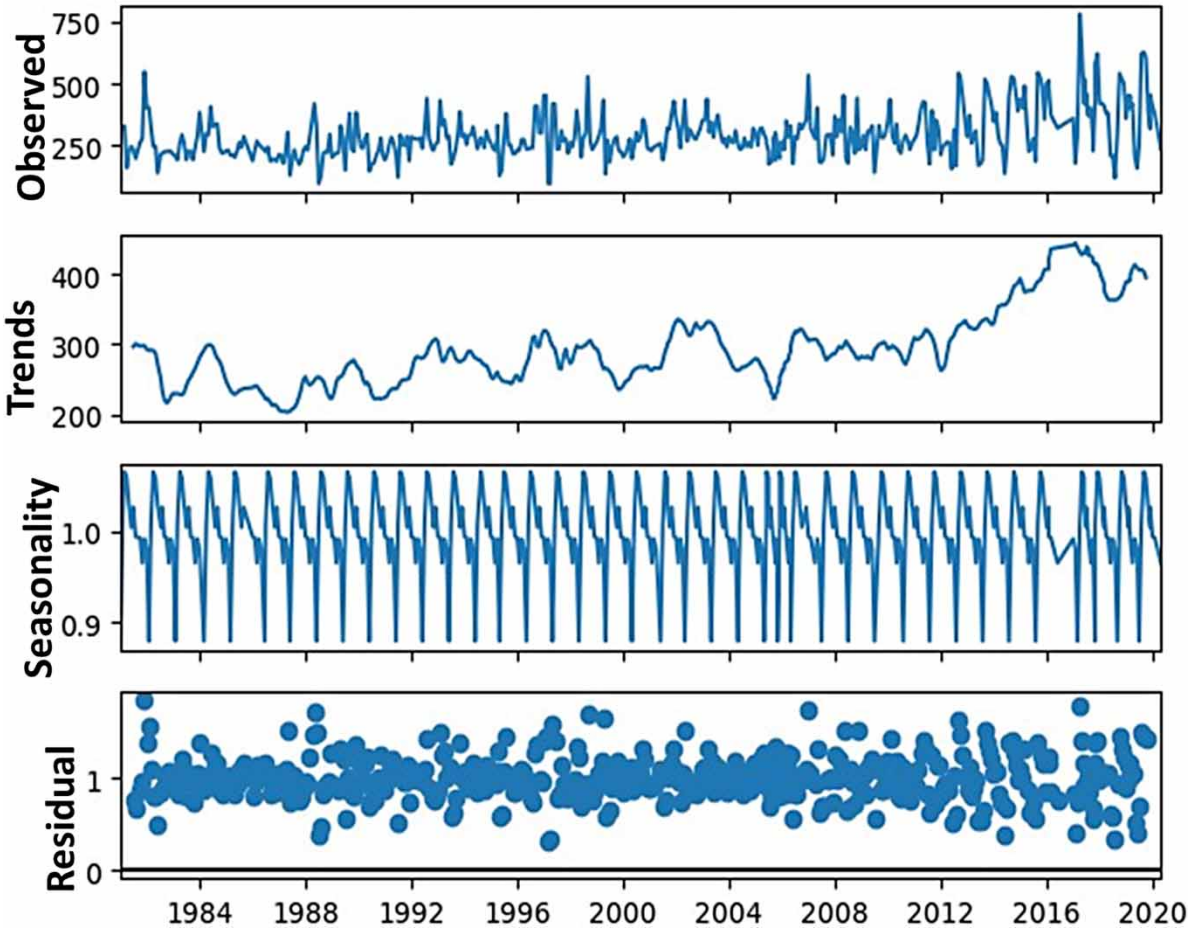

Figure 3 | Monthly distribution of electrical conductivity data from the Sandia hydrological site, Narmada River, classified into observed, trend, seasonality, and residual components.

METHODOLOGY

The Supplementary Material presents a flowchart of the research methodology. The monthly water sample was picked up from the Sandia Ghat site and analyzed by CWC New Delhi, India. The water sample was collected in the first week of the month. Data about water quality for the 40 years from 1981 to 2020 were acquired from the divisional office of CWC Sandia, Madhya Pradesh, India. For this research work, as mentioned previously, the API Keras was used for water quality parameter predictions. It is an open-source framework written in Python for deep learning that is now a part of the TensorFlow platform. Keras was originally developed as independent from TensorFlow, but later on merged with it, starting from version 2.0. Researchers and developers can build and experiment with neural networks with ease due to its user-focused approach and user-responsive functionalities. LSTM, which is a type of recurrent neural network (RNN) architecture, is also used in this study. LSTMs are a specific variant of RNNs designed to address some of the limitations of traditional RNNs when dealing with long sequences and capturing long-term dependencies in data. The LSTM model has been used for groundwater hydrology (Zhang *et al.* 2018; Afzaal *et al.* 2019; Bowes *et al.* 2019; Supreetha *et al.* 2020; Wunsch *et al.* 2021) and rainfall–runoff forecasting (Hu *et al.* 2018; Kratzert *et al.* 2018). The literature pertaining to the use of LSTM for water quality parameters is not much in trend.

Figure 4 shows the typical architecture of the LSTM neural networks. LSTMs are distinguished by the presence of a gated unit, known as the hidden layer, which consists of four interconnected layers that collaborate to generate the cell's output and cell state. These two components are subsequently transmitted to the subsequent hidden layer. In contrast to RNNs, which incorporate only a single neural network layer utilizing the tanh activation function, LSTMs incorporate three logistic

Downloaded from http://iwaponline.com/jwcc/article-pdf/15/3/1172/1394322/jwc0151172.pdf
by guest

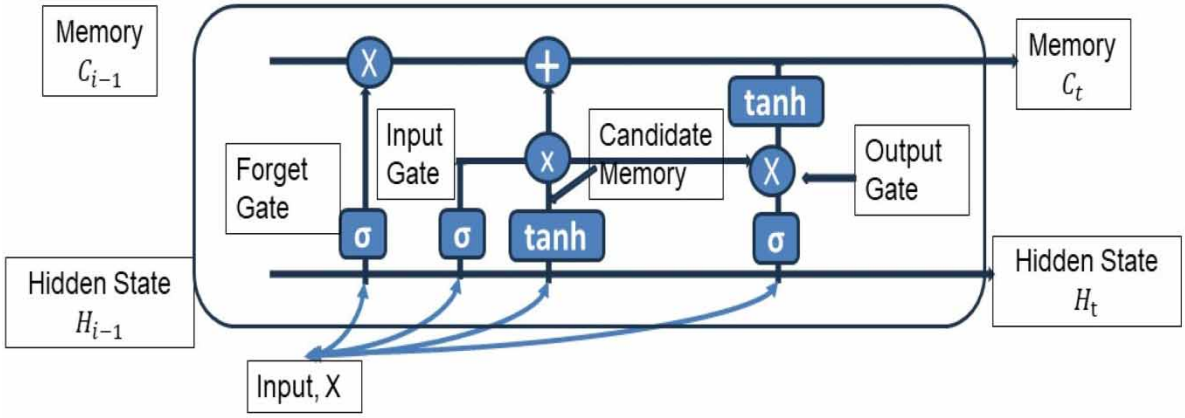

Figure 4 | Typical architecture of LSTM neural networks.

sigmoid gates and one tanh layer. These gates serve the purpose of regulating the flow of information through the cell, deciding what information should be passed on to the next cell and what should be disregarded. The resulting output typically falls within the 0–1 range, where '0' signifies 'discard all' and '1' signifies 'retain all.' LSTMs use the tan-sigmoid function as an activation function for their networks.

In this study, RMSE, coefficient of determination (R^2), Nash–Sutcliffe efficiency (NSE), mean absolute error (MAE), and mean absolute percentage error (MAPE) were selected as performance indicators of the network, and the results are as follows.

$$\text{RMSE} = \sqrt{\frac{\sum_{i=1}^{n} (Y_i - \hat{Y}_i)^2}{n}}$$

where Y_i is the observed (actual) value for the i-th data point, $\hat{Y}_i$ is the predicted value for the i-th data point, and n is the total number of data points.

RMSE provides a measure of how well the predicted values match the actual values. It is expressed in the same units as the original data, which makes it easy to interpret. A lower RMSE indicates a better fit between the predicted and actual values, while a higher RMSE suggests that the model's predictions have larger errors (Lohani *et al.* 2011).

$$\text{Coefficient of determination } (R^2) = \left(1 - \frac{\text{RSS}}{\text{TSS}}\right)$$

where RSS is the sum of squared residuals, and TSS is the total sum of squares.

R^2 measures how well the independent variables account for the variability in the dependent variable. R^2 values range from 0 to 1 (0%–100%). The different R^2 values have the following indications:

- $R^2 = 0$: This means that the independent variables do not explain any of the variability in the dependent variable, and the regression model does not fit the data at all.
- $R^2 = 1$: This indicates that the independent variables perfectly explain all the variability in the dependent variable, and the regression model fits the data perfectly.
- $0 < R^2 < 1$: In practice, R^2 values typically fall between 0 and 1.

A higher R^2 value indicates that a larger proportion of the variance in the dependent variable is explained by the independent variables. For example, an R^2 of 0.80 means that 80% of the variability in the dependent variable is accounted for by the independent variables.

$$\text{NSE} = 1 - \frac{\sum_{t=1}^{n} (O_t - P_t)^2}{\sum_{t=1}^{n} (O_t - \bar{O})^2}$$

Downloaded from http://iwaponline.com/jwcc/article-pdf/15/3/1172/1394322/jwc0151172.pdf
by guest

where O_t denotes the observed values at time t, P_t denotes the simulated or modeled values of the same variable, and $\bar{O}$ denotes the mean of the observed values.

- When NSE equals 1, it indicates a flawless model fit where the simulated values precisely align with the observed values.
- If NSE is greater than 0, it signifies that the model is delivering predictions superior to the average of the observed values.
- When NSE equals 0, it suggests that the model's performance is equivalent to using the mean of the observed values, with no improvement.
- If NSE falls below 0, it implies that the model's predictions are less accurate than those derived from the mean of the observed values.

$$\text{Mean absolute error (MAE)} = (1/n) \times \Sigma|y\_\text{observed} - y\_\text{predicted}|$$

A reduced MAE implies that, on average, the model's predictions closely align with the observed values, reflecting higher accuracy. Conversely, an elevated MAE indicates that the model's predictions exhibit larger absolute discrepancies from the observed values, implying lower accuracy.

$$\text{Mean absolute percentage error (MAPE)} = \frac{1}{n} \times \frac{\Sigma(|(y\_\text{observed} - y\_\text{predicted})}{y\_\text{observed}} \times 100$$

When MAPE is lower, it indicates that the model's predictions exhibit smaller relative errors compared with the observed values, implying greater accuracy in relative terms. Conversely, a higher MAPE implies that the model's predictions display larger relative errors relative to the observed values, suggesting reduced accuracy in relative terms.

RESULTS AND DISCUSSION

A total of ten models were applied for predicting the EC of the Narmada River basin at Sandia hydrological site. Table 3 and Figures 5 represents the fluctuations in various performance metrics of the models during the prediction process. The input shape represents the number of months (in the middle), which was used as input for the network. The batch shape indicates the number of months for which the prediction was achieved for the given LSTM network. A higher R^2 value indicates a better fit. In this table, the R^2 values range from 0.748 to 0.889. Model 8 with the highest R^2 value (0.889) appears to have the best fit. Golian *et al.* (2015) employed R^2 values for discharge prediction goodness-of-fit criteria and a highest value of 0.86 was achieved. Salehnia *et al.* (2017) also used R^2 value as a reliable indicator for drought indices comparison.

Lower RMSE values indicate better predictive accuracy. Model 10 with the lowest RMSE (80.25) is a strong contender for the best model. RMSE has also been used to predict complex wavelet neural networks for daily river-flow predictions (Krishna *et al.* 2011). Nourani *et al.* (2012) used RMSE for calibration and verification of genetic programming neural networks for highlighting best results for different types of watersheds. Other researchers have also used RMSE for flood

Table 3 | Variation of different performance parameters of the models during prediction

S No.	Input shape	Batch shape	R^2	RMSE	NSE	MAE	MAPE (%)
1	(1–3–1)	(1–12–1)	0.845	129.19	0.32	109.06	15
2	(1–4–1)	(1–12–1)	0.878	109.41	0.51	94.14	12
3	(1–5–1)	(1–12–1)	0.833	141.82	0.18	115.96	16
4	(1–6–1)	(1–12–1)	0.825	107.75	0.52	90.86	12
5	(1–7–1)	(1–12–1)	0.872	98.72	0.60	86.92	11
6	(1–8–1)	(1–12–1)	0.748	139.51	0.20	116.62	17
7	(1–9–1)	(1–12–1)	0.842	113.56	0.47	96.44	13
8	(1–10–1)	(1–12–1)	0.889	92.43	0.65	83.04	11
9	(1–11–1)	(1–12–1)	0.835	89.91	0.67	78.77	11
10	(1–12–1)	(1–12–1)	0.853	80.25	0.74	72.27	9

Downloaded from http://iwaponline.com/jwcc/article-pdf/15/3/1172/1394322/jwc0151172.pdf
by guest

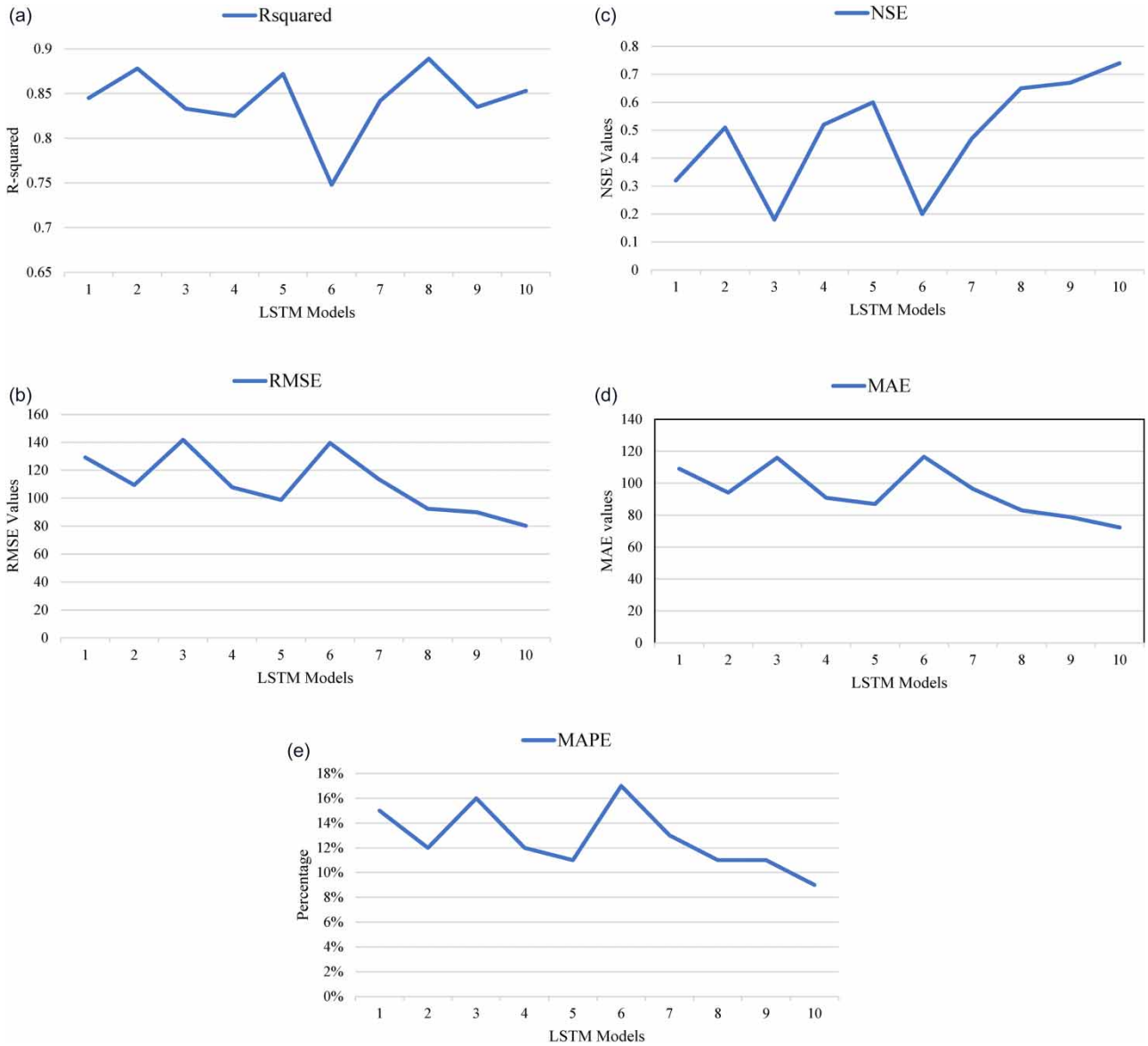

Figure 5 | Variation graphs for the ten LSTM models for: (a) R^2; (b) RMSE values; (c) NSE values; (d) MAE values; and (e) MAPE percentages.

forecasting (Golian *et al.* 2015), change in river topology and vegetation (Watanabe & Kawahara 2016), streamflow predictions (Tegegne *et al.* 2017), and hazard mapping (Kumar *et al.* 2022), among others.

The NSE value that lies above 0.5 can be considered as an optimal one (Quansah *et al.* 2021). The resulting values of NSE lie between 0.18 and 0.74. Model 3 with the least value of NSE, 0.18, does not show much improvement over the observed value. Model 10 with a maximum value of 0.74 performs best followed by Models 9 and 8. Fares *et al.* (2014) obtained values of NSE between 0.65 and 0.74 and found the model's general performance rating to be good. Jiang *et al.* (2015) also obtained values of NSE between 0.71 and 0.90 and found it a satisfactory parameter for accessing performance criteria.

MAE is a great tool to understand the uncertainty in the prediction of a model (Freedman *et al.* 2014). Lower MAE values indicate better performance, as they represent how close the model's predictions are to the actual values. Model 10 has the lowest MAE of 72.27, indicating it has the best predictive performance among the ten models. Model 9 also has a relatively low MAE of 78.77, showing good predictive accuracy. Models 8 and 5 have MAE values in the 80s, indicating reasonable predictive performance. Models 2, 4 and 7 have MAE values in the 90s, indicating decent but slightly less accurate predictions compared with the previous models. Models 3 and 6 have higher MAE of about 116, suggesting that they have less accurate

Downloaded from http://iwaponline.com/jwcc/article-pdf/15/3/1172/1394322/jwc0151172.pdf
by guest

predictions. In summary, Models 10 and 9 perform the best in terms of prediction accuracy, while Models 3 and 6 perform the worst. MAE was also used by previous researchers for rainfall–runoff simulation (Hu *et al.* 2018), monthly stream flow (Bisht *et al.* 2020), hourly flood predictions (Tiwari & Chatterjee 2010), and so on.

Lower MAPE values indicate better predictive accuracy. LSTM Model 10 has the lowest MAPE of 9%, indicating it has the best predictive accuracy among the ten models. This means that, on average, its predictions are only off by 9% from the actual values in terms of percentage error. Models 5, 8, and 9 all have MAPE values of 11%, which also indicates very good predictive accuracy. These models are consistently accurate, with predictions deviating by only 11% from actual values. Accurate precision on a relative scale is demonstrated by Models 2 and 4 with MAPE values of 12%, which is well within the acceptable limits. As far as Models 7 and 3 are concerned, they have MAPE values of 13% and 16%, respectively, which show that these models are slightly less precise than the preceding ones but may still be considered acceptable depending on the application of the EC prediction. This shows that predictions deviating by a higher percentage from the actual values make the models less reliable for monthly prediction. To sum up, Model 10 has emerged with best predictive accuracy, followed closely by Models 5, 8, and 9, which also executed well. Moderate accuracy is achieved with Models 2 and 4, whereas Models 7 and 3 are less accurate than the previous ones. Wilby *et al.* (2003) uses MAPE for performance evaluation of conceptual models in runoff analysis.

In this study, the best-performing model is Model 8 with an R^2 value of 0.89, which is extremely good compared with the various other models proposed by the researchers in recent times. Ubah *et al.* (2021) used artificial neural network (ANN) models (feed-orward multilayer neural networks) for forecasting the EC with the best-performing model having an R^2 value of 0.95. Other researchers also used the feed-forward ANN and statistical methods for EC prediction with an R^2 value of 0.83 (Satish *et al.* 2022). Sunori *et al.* (2023) used a regression tree model known as a general regression neural network (GRNN) for prediction of EC and found it satisfactory for forecasting.

CONCLUSION

In this paper, a comprehensive study was conducted to understand the climate-change impacts on parameters associated with water quality with a special focus on EC at the Sandia hydrological observation site located on the Narmada River basin, Central India. It aimed at helping to bridge the gap between understanding the intricate relationship of water quality with climate change using artificial neural networks as a supporting tool. EC is a crucial parameter to affect the quality. For prediction of EC in the context of climate change, LSTM models were used in this study. A total of ten models based on input parameters were introduced and recently used for water quality prediction work. A total of five performance criteria were used, consisting of RMSE, coefficient of determination (R^2), NSE, MAE, and MAPE. Among the models, Model 8 performs the best with the highest R^2 value of 0.889, demonstrating excellent predicting capability. With the lowest MAE of 72.27 and MAPE of 9%, Model 10 also performs well. The MAPE value of 11% exhibited by Models 5, 8, and 9 also shows consistent and better accuracy. These results show the performance efficiency of the LSTM model in predicting the EC for the observation site is quite acceptable for decision-making and assessing the impact of climate change. One of the limitations of the model is that it is as accurate as the data obtained from the site. Because the collection of data and testing are manual, there may be some discrepancies in the results produced. Further studies can be carried out for different parameters, different neural networks, and data-processing tools like wavelets.

DATA AVAILABILITY STATEMENT

All relevant data are included in the paper or its Supplementary Information.

CONFLICT OF INTEREST

The authors declare there is no conflict.

REFERENCES

Afzaal, H., Farooque, A. A., Abbas, F., Acharya, B. & Esau, T. 2019 Groundwater estimation from major physical hydrology components using artificial neural networks and deep learning. *Water* **12** (1), 5. https://doi.org/10.3390/w12010005.

Bhagwat, P. P. & Maity, R. 2014 Development of HydroClimatic Conceptual Streamflow (HCCS) model for Tropical River basin. *Journal of Water and Climate Change* **5** (1), 36–60. https://doi.org/10.2166/wcc.2013.015.

Downloaded from http://iwaponline.com/jwcc/article-pdf/15/3/1172/1394322/jwc0151172.pdf
by guest

Bisht, D. S., Mohite, A. R., Jena, P. P., Khatun, A., Chatterjee, C., Raghuwanshi, N. S., Singh, R. & Sahoo, B. 2020 Impact of climate change on streamflow regime of a large Indian river Basin using a novel monthly hybrid bias correction technique and a conceptual modeling framework. *Journal of Hydrology* **590**, 125448. https://doi.org/10.1016/j.jhydrol.2020.125448.

Bowes, B. D., Sadler, J. M., Morsy, M. M., Behl, M. & Goodall, J. L. 2019 Forecasting groundwater table in a flood prone coastal city with long short-term memory and recurrent neural networks. *Water* **11** (5), 1098. https://doi.org/10.3390/w11051098.

Corwin, D. L. & Lesch, S. M. 2005 Apparent soil electrical conductivity measurements in agriculture. *Computers and Electronics in Agriculture* **46** (1–3), 11–43. https://doi.org/10.1016/j.compag.2004.10.005.

Delpla, I., Jung, A.-V., Baures, E., Clement, M. & Thomas, O. 2009 Impacts of climate change on surface water quality in relation to drinking water production. *Environment International* **35** (8), 1225–1233. https://doi.org/10.1016/j.envint.2009.07.001.

Dile, Y. T., Tekleab, S., Ayana, E. K., Gebrehiwot, S. G., Worqlul, A. W., Bayabil, H. K., Yimam, Y. T., Tilahun, S. A., Daggupati, P., Karlberg, L. & Srinivasan, R. 2018 Advances in water resources research in the Upper Blue Nile basin and the way forward: a review. *Journal of Hydrology* **560**, 407–423. https://doi.org/10.1016/j.jhydrol.2018.03.042.

Doocy, S., Daniels, A., Murray, S. & Kirsch, T. D. 2013 The human impact of floods: a historical review of events 1980–2009 and systematic literature review. *PLoS Currents Disasters* **5** (16 April). doi:10.1371/currents.dis.f4deb457904936b07c09daa98ee8171a.

Fares, A., Awal, R., Michaud, J., Chu, P.-S., Fares, S., Kodama, K. & Rosener, M. 2014 Rainfall-runoff modeling in a flashy tropical watershed using the distributed HL-RDHM model. *Journal of Hydrology* **519**, 3436–3447. https://doi.org/10.1016/j.jhydrol.2014.09.042.

Freedman, F. R., Pitts, K. L. & Bridger, A. F. C. 2014 Evaluation of CMIP climate model hydrological output for the Mississippi River Basin using GRACE satellite observations. *Journal of Hydrology* **519**, 3566–3577. https://doi.org/10.1016/j.jhydrol.2014.10.036.

Golian, S., Fallahi, M. R., Behbahani, S. M., Sharifi, S. & Sharma, A. 2015 Real-time updating of rainfall threshold curves for flood forecasting. *Journal of Hydrologic Engineering* **20** (4), 04014059. https://doi.org/10.1061/(ASCE)HE.1943-5584.0001049.

Gomaa, M. M., Melegy, A., Metwaly, H. & Hassan, S. 2020 Geochemical and electrical characterization of heavy metals in contaminated soils. *Heliyon* **6** (9), e04954. https://doi.org/10.1016/j.heliyon.2020.e04954.

Goyal, M. K. & Surampalli, R. Y. 2018 Impact of climate change on water resources in India. *Journal of Environmental Engineering* **144** (7), 04018054. https://doi.org/10.1061/(ASCE)EE.1943-7870.0001394.

Heddam, S. & Kisi, O. 2018 Modelling daily dissolved oxygen concentration using least square support vector machine, multivariate adaptive regression splines and M5 model tree. *Journal of Hydrology* **559**, 499–509. https://doi.org/10.1016/j.jhydrol.2018.02.061.

Hu, C., Wu, Q., Li, H., Jian, S., Li, N. & Lou, Z. 2018 Deep learning with a long short-term memory networks approach for rainfall-runoff simulation. *Water* **10** (11), 1543. https://doi.org/10.3390/w10111543.

Jiang, Y., Liu, C., Li, X., Liu, L. & Wang, H. 2015 Rainfall-runoff modeling, parameter estimation and sensitivity analysis in a semiarid catchment. *Environmental Modelling and Software* **67**, 72–88. https://doi.org/10.1016/j.envsoft.2015.01.008.

Kratzert, F., Klotz, D., Brenner, C., Schulz, K. & Herrnegger, M. 2018 Rainfall–runoff modelling using Long Short-Term Memory (LSTM) networks. *Hydrology and Earth System Sciences* **22** (11), 6005–6022. https://doi.org/10.5194/hess-22-6005-2018.

Krishna, B., Rao, Y. R. S. & Nayak, P. C. 2011 Time series modeling of river flow using wavelet neural networks. *Journal of Water Resource and Protection* **3** (1), 50–59. https://doi.org/10.4236/jwarp.2011.31006.

Kumar, C. P. 2016 Impact of climate change on groundwater resources. In: *Handbook of Research on Climate Change Impact on Health and Environmental Sustainability* (Dinda, S., ed.), IGI Global, Hershey, PA, USA, pp. 196–221. http://dx.doi.org/10.4018/978-1-4666-8814-8.ch010.

Kumar, N., Poonia, V., Gupta, B. B. & Goyal, M. K. 2021 A novel framework for risk assessment and resilience of critical infrastructure towards climate change. *Technological Forecasting and Social Change* **165**, 120532. https://doi.org/10.1016/j.techfore.2020.120532.

Kumar, P., Garg, V., Mittal, S. & Murthy, Y. V. N. K. 2022 GIS-based hazard and vulnerability assessment of a torrential watershed. *Environment, Development and Sustainability* **24**, 921–951. https://doi.org/10.1007/s10668-021-01476-z.

Lau, A. M. P., Ferreira, F. J. F., Stevanato, R. & da Rosa Filho, E. F. 2019 Geophysical and physicochemical investigations of an area contaminated by tannery waste: a case study from southern Brazil. *Environmental Earth Sciences* **78** (16), 517. https://doi.org/10.1007/s12665-019-8536-1.

Lohani, A. K., Goel, N. K. & Bhatia, K. K. S. 2011 Comparative study of neural network, fuzzy logic and linear transfer function techniques in daily rainfall-runoff modelling under different input domains. *Hydrological Processes* **25** (2), 175–193. https://doi.org/10.1002/hyp.7831.

Mauser, W. & Bach, H. 2009 PROMET – large scale distributed hydrological modelling to study the impact of climate change on the water flows of mountain watersheds. *Journal of Hydrology* **376** (3–4), 362–377. https://doi.org/10.1016/j.jhydrol.2009.07.046.

Mishra, S. S. & Nagarajan, R. 2010 Morphometric analysis and prioritization of subwatersheds using GIS and remote sensing techniques: a case study of Odisha, India. *International Journal of Geomatics and Geosciences* **1** (3), 501–510.

Mohammed, R. & Scholz, M. 2018 Climate change and anthropogenic intervention impact on the hydrologic anomalies in a semi-arid area: Lower Zab River Basin, Iraq. *Environmental Earth Sciences* **77** (10), 357. https://doi.org/10.1007/s12665-018-7537-9.

Nourani, V., Komasi, M. & Alami, M. T. 2012 Hybrid wavelet–genetic programming approach to optimize ANN modeling of rainfall–runoff process. *Journal of Hydrologic Engineering* **17** (6), 724–741. https://doi.org/10.1061/(ASCE)HE.1943-5584.0000506.

Pal, M., Samal, N. R., Roy, P. K. & Roy, M. B. 2015 Electrical conductivity of lake water as environmental monitoring – a case study of Rudrasagar Lake. *IOSR Journal of Environmental Science, Toxicology and Food Technology* **9** (3), 66–71. https://doi.org/10.9790/2402-09316671.

Downloaded from http://iwaponline.com/jwcc/article-pdf/15/3/1172/1394322/jwc0151172.pdf
by guest

Quansah, J. E., Naliaka, A. B., Fall, S., Ankumah, R. & El Afandi, G. 2021 Assessing future impacts of climate change on streamflow within the Alabama River Basin. *Climate* **9** (4), 55. https://doi.org/10.3390/cli9040055.

Rai, S. & Singh, R. 2015 Environmental impact assessment of a rural road project: network and matrix method. *International Journal of Scientific Research in Science, Engineering and Technology* **1** (4), 170–179.

Salehnia, N., Alizadeh, A., Sanaeinejad, H., Bannayan, M., Zarrin, A. & Hoogenboom, G. 2017 Estimation of meteorological drought indices based on AgMERRA precipitation data and station-observed precipitation data. *Journal of Arid Land* **9** (6), 797–809. https://doi.org/10.1007/s40333-017-0070-y.

Satish, N., Anmala, J., Rajitha, K. & Varma, M. R. R. 2022 Prediction of stream water quality in Godavari River Basin, India using statistical and artificial neural network models. *H2Open Journal* **5** (4), 621–641. https://doi.org/10.2166/h2oj.2022.019.

Sunori, S. K., Negi, P. B., Bhawana & Juneja, P. 2023 AI & ML based prediction of electrical conductivity of water. In: *2nd International Conference on Sustainable Computing and Data Communication Systems, ICSCDS 2023 – Proceedings*, IEEE, Piscataway, NJ, USA, pp. 487–491. https://doi.org/10.1109/ICSCDS56580.2023.10104788.

Supreetha, B. S., Shenoy, N. & Nayak, P. 2020 Lion algorithm-optimized long short-term memory network for groundwater level forecasting in Udupi District, India. *Applied Computational Intelligence and Soft Computing* **2020**, 8685724. https://doi.org/10.1155/2020/8685724.

Tegegne, G., Park, D. K. & Kim, Y. 2017 Comparison of hydrological models for the assessment of water resources in a data-scarce region, the Upper Blue Nile River Basin. *Journal of Hydrology: Regional Studies* **14**, 49–66. https://doi.org/10.1016/j.ejrh.2017.10.002.

Tiwari, M. K. & Chatterjee, C. 2010 Development of an accurate and reliable hourly flood forecasting model using wavelet–bootstrap–ANN (WBANN) hybrid approach. *Journal of Hydrology* **394** (4), 458–470. https://doi.org/10.1016/j.jhydrol.2010.10.001.

Tiwari, D. K., Tiwari, H. L. & Nateriya, R. 2022 Runoff modeling in Kolar River basin using hybrid approach of wavelet with artificial neural network. *Journal of Water and Climate Change* **13** (2), 963–974. https://doi.org/10.2166/wcc.2021.246.

Ubah, J. I., Orakwe, L. C., Ogbu, K. N., Awu, J. I., Ahaneku, I. E. & Chukwuma, E. C. 2021 Forecasting water quality parameters using artificial neural network for irrigation purposes. *Scientific Reports* **11** (1), 24438. https://doi.org/10.1038/s41598-021-04062-5.

van Allemann, S., Dippenaar, M. A. & Olivier, J. 2019 A laboratory study of the leachate composition of selected metals in cemeteries (South Africa). *Environmental Earth Sciences* **78** (16), 518. https://doi.org/10.1007/s12665-019-8521-8.

Watanabe, Y. & Kawahara, Y. 2016 UAV photogrammetry for monitoring changes in river topography and vegetation. *Procedia Engineering* **154**, 317–325. https://doi.org/10.1016/j.proeng.2016.07.482.

Wilby, R. L., Abrahart, R. J. & Dawson, C. W. 2003 Detection of conceptual model rainfall–runoff processes inside an artificial neural network. *Hydrological Sciences Journal* **48** (2), 163–181. https://doi.org/10.1623/hysj.48.2.163.44699.

Wunsch, A., Liesch, T. & Broda, S. 2021 Groundwater level forecasting with artificial neural networks: a comparison of long short-term memory (LSTM), convolutional neural networks (CNNs), and non-linear autoregressive networks with exogenous input (NARX). *Hydrology and Earth System Sciences* **25** (3), 1671–1687. https://doi.org/10.5194/hess-25-1671-2021.

Zhang, J., Zhu, Y., Zhang, X., Ye, M. & Yang, J. 2018 Developing a Long Short-Term Memory (LSTM) based model for predicting water table depth in agricultural areas. *Journal of Hydrology* **561**, 918–929. https://doi.org/10.1016/j.jhydrol.2018.04.065.

First received 17 September 2023; accepted in revised form 6 February 2024. Available online 19 February 2024

Downloaded from http://iwaponline.com/jwcc/article-pdf/15/3/1172/1394322/jwc0151172.pdf
by guest